Investigation into the formation of heteronuclear clusters of formula [{Ru$_6$C(CO)$_{16}$Ag$_2$X}$_2$]$^{2-}$ (X = Cl, Br or I)

Danielle M. Chisholm,[1] **J. Scott McIndoe,**[1,3] **Gabriella Bodizs,**[2] **Wee Han Ang,**[2] **Rosario Scopelliti,**[2] **and Paul J. Dyson**[2]

Reaction of [Ru$_6$C(CO)$_{16}$]$^{2-}$ with an excess of AgX (X = Cl, Br or I) affords heteronuclear clusters of formula [{Ru$_6$C(CO)$_{16}$Ag$_2$X}$_2$]$^{2-}$ in 80% yield, which for X = I and X = Br/Cl were crystallographically characterised. The formation of the cluster was followed in solution using electrospray ionisation mass spectrometry (ESI-MS), which revealed the presence of a wide range of clusters with the general formula [{Ru$_6$C(CO)$_{16}$}$_x$Ag$_y$X$_z$]$^{(2x-y+z)-}$ where $x = 1$ or 2, $y = 1, 2, 3$ or 4 and $z = 0, 1$ or 2. The high yield of the product despite the evident complicated solution speciation is attributed to selective crystallisation of the observed compound driving the equilibrium toward this product.

KEY WORDS: Carbonyl cluster; ruthenium; silver; mass spectrometry; electrospray ionisation.

INTRODUCTION

Carbide-centred penta- and hexaruthenium carbonyl cluster have proven to be excellent and stable precursors for systematic synthesis of organo-ligand modified systems [1] and higher nuclearity heteronuclear clusters [2]; their chemistry has been reviewed [3]. The use of mercury reagents to connect

[1]Department of Chemistry, University of Victoria, P.O. Box 3065Victoria, BC, Canada V8W 3V6.
[2]Institut des Sciences et Ingénierie Chimiques, Ecole Polytechnique Fédérale de Lausanne (EPFL), CH-1015, Lausanne, Switzerland.
[3]To whom correspondence should be addressed. E-mail: mcindoe@uvic.ca

cluster units has been widely used [4] and successfully applied to the Ru_6C system. Specifically, the reaction of $Hg(CF_3CO_2)_2$ or $HgCl_2$ with two equivalents of $[Ru_6C(CO)_{16}]^{2-}$ in CH_2Cl_2 for 15 min affords $[\{Ru_6C(CO)_{16}\}_2Hg]^{2-}$ in high yield, in which two Ru_6C units are held together by a single mercury centre (Scheme 1) [5]. Using equimolar quantities of $Hg(CF_3CO_2)_2$ and $[Ru_6C(CO)_{16}]^{2-}$ yields an uncharacterised polymeric material. The structure of a closely related thallium cluster, *viz.* $[\{Ru_6C(CO)_{16}\}_2Tl]^-$, has also been reported [6]. Closely related to both $[\{Ru_6C(CO)_{16}\}_2Hg]^{2-}$ and $[\{Ru_6C(CO)_{16}\}_2Tl]^-$, and presumably the uncharacterised polymeric material obtained from the reaction of $[Ru_6C(CO)_{16}]^{2-}$ with $Hg(CF_3CO_2)_2$, at least in terms of structure, is the silver-bridged self-assembled polymeric material $[AgRu_6C(CO)_{16}]^-_\infty$, isolated from the reaction of $[Ru_6C(CO)_{16}]^{2-}$ with $AgNO_3$ [7].

The copper connected cluster $[\{Ru_6C(CO)_{16}Cu_2Cl\}_2]^{2-}$, an analogue of those disclosed in this paper (see below) has been isolated from the reaction of $[Ru_6C(CO)_{16}]^{2-}$ with an excess of CuCl in thf [8]. This cluster has been shown to act as a precursor to high-performance, bimetallic nanoparticle catalysts supported inside mesoporous silica [9]. The pentaruthenium-carbide
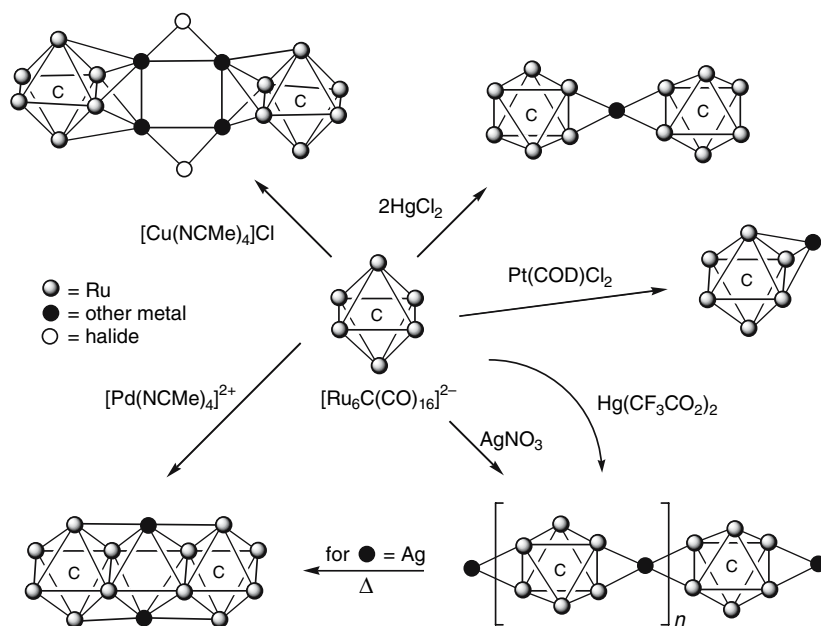
Scheme 1. Examples of heteronuclear cluster synthesis using $[Ru_6C(CO)_{16}]^{2-}$ as a precursor: non-halide ligands omitted for clarity.

cluster $[Ru_5C(CO)_{14}]^{2-}$ has also been widely used as a precursor to heteronuclear systems, usually involving capping of the square-face of the cluster *via* redox condensation reactions to afford products with an octahedral mixed-metal core [10]. However, reaction of $[Ru_5C(CO)_{14}]^{2-}$ with three equivalents of $AgBF_4$ affords $[\{Ru_6C(CO)_{16}\}_2Ag_3Cl]^{2-}$ in which the Ag_3Cl unit bridge the two ruthenium polyhedra *via* triangular faces [11]. $[Ru_6C(CO)_{16}]^{2-}$ also reacts readily with mononuclear metal fragments, such as with $PtCl_2(COD)$ (COD = 1,5-cyclooctadiene) to produce $PtRu_6C(CO)_{16}(COD)$ [12].

Heteronuclear clusters based on ruthenium systems, which contain one or more non-Group 8 metal atoms remains an active area of research. The presence of the other metals introduces a polarity into the cluster framework that produces metal geometries not observed in homometal clusters, but also has implications in catalysis [13]. Notably, recent attention has focused on using these well defined and characterised heteronuclear clusters as precursors to supported nanoparticle materials, which demonstrate some impressive catalytic properties [14].

In this paper we structurally describe a new heteronuclear cluster and examine the solution speciation over the course of the reaction using electrospray ionisation mass spectrometry.

EXPERIMENTAL

All manipulations were performed under an inert atmosphere of dry nitrogen using standard Schlenk techniques. Appropriate silver halides were prepared from $AgNO_3$ by reaction with the potassium or sodium halides. $[Bu_4N]_2[Ru_6C(CO)_{16}]$ was prepared in two steps, first involving the synthesis of $Ru_6C(CO)_{17}$ from $Ru_3(CO)_{12}$ [15], followed by reductive decarbonylation of $Ru_6C(CO)_{17}$ to the required dianion using methanolic KOH, with concomitant metathesis of the cation [16]. Infrared spectra were recorded on a Perkin–Elmer 2000 FT-IR spectrometer. Electrospray ionisation mass spectra were collected using a Micromass QTof *micro* instrument. Capillary voltage was set at 2900 V, source and desolvation gas temperatures were at 40 and 100°C, respectively. Cone voltage was set at 5 V for all spectra. Samples were infused *via* syringe pump at 5–10 μL min^{-1}. EDESI-MS (/MS) spectra were collected using published procedures [17].

Synthesis of $[\{Ru_6C(CO)_{16}Ag_2X\}_2]^{2-}$ (X = I, Br or Cl)

A 5-fold excess of freshly prepared AgX (5 mol equiv.) was added to $[Bu_4N]_2[Ru_6C(CO)_{16}]$ (60 mg) in thf (25 ml). The reaction mixture was stirred at room temperature for 1–4 h, during which time IR spectroscopy

indicated that the reaction was complete. The product was isolated by precipitation and filtration through Celite following the addition of hexane to the reaction mixture (yield, *ca.* 80%). IR υ_{CO} (CH_2Cl_2): 2046 (w, sh), 1991 (vs), 1942 (w). ESI-MS (MeOH).

Crystals of $[Bu_4N]_2[\{Ru_6C(CO)_{16}Ag_2I\}_2]$ and $[Bu_4N]_2[\{Ru_6C(CO)_{16}Ag_2X\}_2]$ (X = Br: Cl, 50: 50) were grown in a few days from thf-hexane solution at 4°C.

Structural characterisation in the solid state

Relevant details about the structure refinements are compiled in Table I and selected bond distances and angles are given in the figure captions. Data collection was performed on a MAR325 IPDS at 140(2) K and data

Table I. Crystallographic data for $[Bu_4N]_2[\{Ru_6C(CO)_{16}Ag_2X\}_2]$ (X = Cl and Br)

Compound	$[Bu_4N]_2[\{Ru_6C(CO)_{16}Ag_2X\}_2]$ (X = Cl and Br)
Formula	$C_{34}Ag_4BrClO_{32}Ru_{12}\cdot(C_{16}H_{36}N)_2\cdot C_4H_8O$
*F*w	3237.04
Crystal system	Triclinic
Space group	$P\bar{1}$
A (Å)	10.1035(17)
B (Å)	14.227(2)
C (Å)	16.658(4)
α (°)	82.877(15)
β (°)	83.317(16)
γ (°)	84.357(13)
Volume (Å³)	2351.3(7)
Z	1
D_{calc} (g cm⁻³)	2.286
μ (mm⁻¹)	3.205
F(000)	1546
Temp (K)	140(2)
Wavelength (Å)	0.71073
Measured reflns	15597
Unique reflns	7955
Unique reflns [$I > 2\sigma(I)$]	6388
No. of data/restraints/parameters	7955/55/582
R^a [$I > 2\sigma(I)$]	0.0411
$wR2^a$ (all data)	0.1226
GooF^b	1.101

[a] $R = \mathrm{T}||F_o|-|F_c||/\mathrm{T}|F_o|$, $wR2 = \{\mathrm{T}[w(F_o^2-F_c^2)2]/\mathrm{T}[w(F_o^2)^2]\}^{1/2}$.
[b] GooF $= \{\mathrm{T}[w(F_o^2-F_c^2)2]/(n-\mathrm{p})\}^{1/2}$ where *n* is the number of data and *p* is the number of parameters refined.

reduction was performed using CrysAlis RED [18]. The structures were solved by Direct methods using SHELXS−97 [19], and refined by full-matrix least-squares refinement (against F^2) using SHELXTL software [20]. All non-hydrogen atoms were refined anisotropically while hydrogen atoms were placed in their geometrically generated positions and refined using the riding model. SIMU and DELU restraints were applied for the disordered thf solvent molecule. Empirical absorption corrections were applied using DELABS [21], and graphical representations of the structures were made with Diamond [22]. CCDC 624233 contains the supplementary crystallographic data for this paper. These data can be obtained free of charge from The Cambridge Crystallographic Data Centre *via* www.ccdc.cam.ac.uk/ data_request/cif.

RESULTS AND DISCUSSION

The heteronuclear clusters $[\{Ru_6C(CO)_{16}Ag_2X\}_2]^{2-}$ (X = Cl, Br or I) are readily prepared in good yield, *ca.* 80%, from the reaction of $[Ru_6C(CO)_{16}]^{2-}$ with a 5-fold excess of AgX in thf. A characteristic peak in the IR υ_{CO} region at 1991 cm^{-1} corresponds to the product, and *in situ* monitoring of the carbonyl stretches for the precursor cluster clearly shows when the reaction has reached completion, typically between 1 and 4 h. Crystals of the iodide containing cluster $[\{Ru_6C(CO)_{16}Ag_2I\}_2]^{2-}$ were grown from thf-hexane solution at 4°C. Attempts to crystallize $[\{Ru_6C(CO)_{16}Ag_2Br\}_2]^{2-}$ from thf-hexane solution resulted in crystallisation of the mixed halide species $[\{Ru_6C(CO)_{16}Ag_2X\}_2]^{2-}$ (X = Br: Cl, 50: 50), due to the presence of chloride impurities in the $[Ru_6C(CO)_{16}]^{2-}$ salt, prepared *via* metathesis with tetrabutylammonium chloride.

The structures of $[\{Ru_6C(CO)_{16}Ag_2I\}_2]^{2-}$ and $[\{Ru_6C(CO)_{16}Ag_2X\}_2]^{2-}$ (X = Cl and Br) are shown in Figs. 1 and 2, respectively, key bond parameters for $[\{Ru_6C(CO)_{16}Ag_2X\}_2]^{2-}$ (X = Cl and Br) are given in the caption to Fig. 3. Due to the poor quality of the crystals of $[\{Ru_6C(CO)_{16}Ag_2I\}_2]^{2-}$ only the gross structural features can be described and bond lengths and angles should be treated with caution, however, the metal cores of both clusters are closely related, as can be appreciated from Fig. 3 which highlights the geometry of the metal polyhedral skeleton. Both structures are based on two Ru_6C octahedral units connected *via* a planar Ag_4X_2 unit (where X corresponds to iodide in $[\{Ru_6C(CO)_{16}Ag_2I\}_2]^{2-}$ and to Br/Cl in the other cluster). The structural core is analogous to that observed in $[\{Ru_6C(CO)_{16}Cu_2Cl\}_2]^{2-}$ [8]. Note that crystallography cannot distinguish between Cl and Br disorder in the same anion and a mixture of Cl_{2-} and Br_{2-} containing cluster anions disordered on the same site. In fact all three
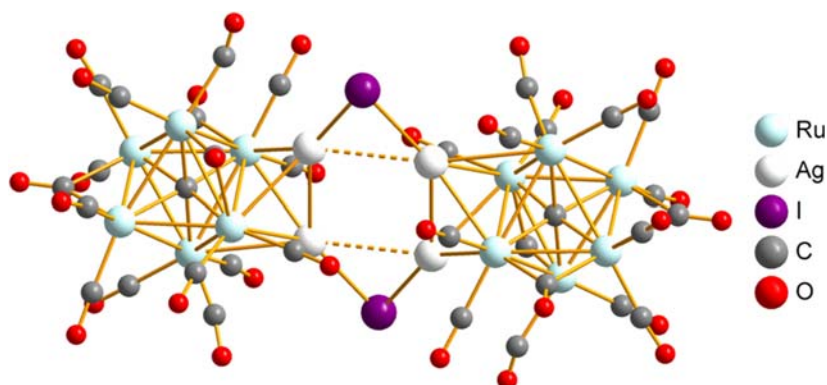
Fig. 1. Ball and stick representation of $[\{Ru_6C(CO)_{16}Ag_2I\}_2]^{2-}$; counter cations are omitted for clarity.

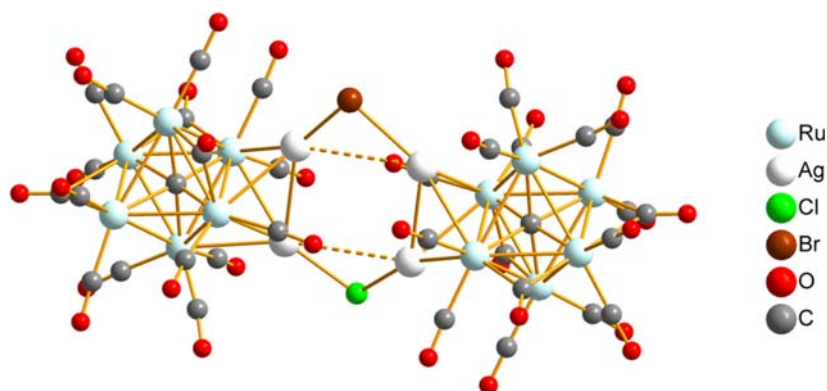**Fig. 2.** Ball and stick representation of $[\{Ru_6C(CO)_{16}Ag_2X\}_2]^{2-}$ (X = Cl and Br). The counter cations and solute are omitted for clarity. The Br and Cl atoms are disordered and the disordered positions are omitted.

clusters may be present in the crystal, and the ESI-MS results reported later in the paper lead us to suspect that this is probably the case.

One face of each Ru_6C unit is asymmetrically capped by one of the Ag atoms with the other Ag atom capping the triruthenium face in a manner similar to that observed in $[Ru_6Cu_2C(CO)_{16}(MeCN)_2]$ [23]. Such an arrangement causes a distortion to the Ru_6C octahedron in which the edge bridged by both Ag atoms is elongated [3.1709(10) Å] relative to the other Ru–Ru vectors. The Ag–Ag distances linking the two Ru_6C units [3.7490(11) Å] is longer than the distance of the two Ag atoms bonded to

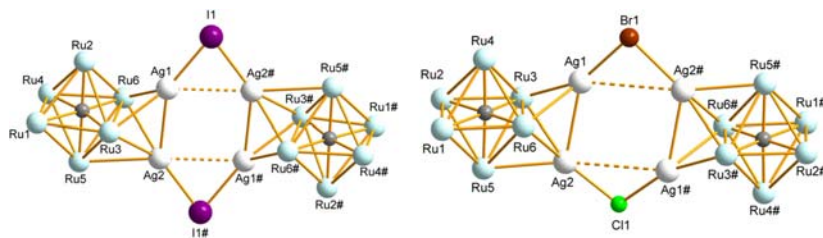**Fig. 3.** Ball and stick representation of the bimetallic cluster core of $[\{Ru_6C(CO)_{16}Ag_2I\}_2]^{2-}$ (left) and $[\{Ru_6C(CO)_{16}Ag_2X\}_2]^{2-}$ (X = Cl and Br) (right). Key bond lengths (Å) and angles (°) for $[\{Ru_6C(CO)_{16}Ag_2X\}_2]^{2-}$ (X = Cl and Br) (the interstitial C is denoted by C36): Ru–Ru_{ave}, 2.917; Ru–Ag_{ave}, 2.834; Ru–$C36_{ave}$, 2.064; Ag_1–Ag_2, 2.9609(9); Ag_1–Ag_2#, 3.7490(11); (Ru–$CO_{terminal}$)$_{ave}$, 1.903; (Ru–$CO_{bridging}$)$_{ave}$, 2.108; (C–$O_{terminal}$)$_{ave}$, 1.134; (C–$O_{bridging}$)$_{ave}$, 1.160, Ag–Br_{ave}, 2.611; Ag–Cl_{ave}, 2.435; Ag_1–Br_1–Ag_2#, 91.8(2) ; Ag_2–Cl_1–Ag_1#, 100.7(7).

the same Ru_6C unit [2.9609(9) Å] and is beyond that which generally constitutes a Ag–Ag bond. Such distortions are also present in the related copper system [8] and even greater distortions have been observed in other Ru_6C-based clusters where sterically demanding ligands are purported to be responsible for the elongation of one or more bond lengths [24].

Reaction insights from mass spectrometry

The reaction between AgX and $[PPN]_2[Ru_6C(CO)_{16}]$ (PPN = bis-{triphenylphosphino}imimium) was tracked using electrospray ionisation mass spectrometry (ESI-MS) [25]. ESI-MS has made the analysis of high nuclearity anionic clusters routine; it is a soft ionisation technique capable of analysing complex mixtures, providing a single unfragmented peak for each species present in solution [26].

Immediately after mixing of the cluster dianion and silver salt in THF, a drop of the solution was extracted, diluted in CH_2Cl_2 and a negative-ion mass spectrum collected, using conditions suited to the analysis of sensitive organometallic complexes (source and desolvation gas at ambient temperature, very low cone voltage). The reaction solution was reexamined at 30 min intervals until no change in solution speciation was observed (about 1.5 h). Representative spectra are shown in Fig. 4. ESI-MS readily discriminates between monoanionic and dianionic complexes (peaks in the isotope patterns are 1 or 0.5 m/z apart, respectively), but the presence of any neutral complexes will go undetected. For brevity and clarity, "Θ" is henceforth used to represent $Ru_6C(CO)_{16}$.

In the case of the reaction with silver iodide, at $t \sim 2$ min, the solution consists mostly of starting material, $[\Theta]^{2-}$ at 534 m/z (due to the very soft
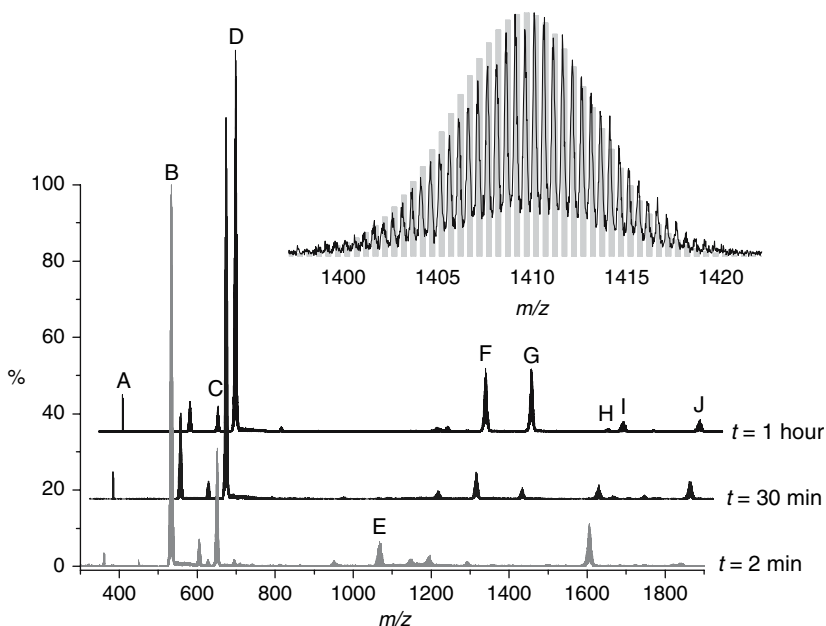
Fig. 4. Negative-ion ESI-MS from the reaction AgI + [PPN]$_2$[Θ]. Peaks in the spectrum correspond to A = [AgI$_2$]$^-$, B = [Θ]$^{2-}$, C = [ΘAgCl]$^{2-}$, D = [ΘAgI]$^{2-}$, E = [HΘ]$^-$, F = [{ΘAg}$_2$AgI]$^{2-}$, G = [{ΘAg$_2$I}$_2$]$^{2-}$/[ΘAg$_2$I]$^-$, H = [Θ(PPN)]$^{2-}$, I = [ΘAg$_3$I$_2$]$^-$, J = [ΘAgI(PPN)]$^-$. The inset shows the experimental and theoretical isotope patterns for [{ΘAg$_2$I}$_2$]$^{2-}$; assignments of the other peaks in the spectrum were carried out on the same basis. The broadness of the isotope pattern is a function of the presence of the large number of polyisotopic metal atoms present.

ionisation conditions, a monoanionic peak is also seen at 1606 m/z due to the dianion associated with the PPN monocation); some protonated cluster, [HΘ]$^-$, is evident at 1069 m/z. Also appearing is a peak at 651 m/z, which may be readily assigned to [ΘAgI]$^{2-}$. A small amount of [ΘAgCl]$^{2-}$ can also be observed; the chloride ion is probably residual from the synthesis of the [PPN]$_2$[Θ] (cf. the X-ray structure containing Cl and Br ligands). Also visible in the spectra at low m/z are peaks due to I$^-$ and [AgI$_2$]$^-$. A very small quantity of [ΘAg]$^-$ can also be discerned in the spectrum (not labelled in the figure).

After 30 min, [Θ]$^{2-}$ has diminished considerably, mostly replaced by [ΘAgI]$^{2-}$, now the base peak in the spectrum. New higher nuclearity species have also appeared; these include [{ΘAg}$_2$AgI]$^{2-}$ at 1292 m/z, [ΘAg$_2$I]$^-$ at 1410 m/z, and [ΘAg$_3$I$_2$]$^-$ at 1646 m/z. After an hour, changes are essentially in intensity rather than speciation. The starting cluster has nearly disappeared

and over 95% of the intensity of the spectrum is due to derivatives of the starting material bonded to differing amounts of Ag and I.

Interestingly, the nature of the peak at 1410 m/z changes, with the peak changing from a 1− to a 2− ion (Fig. 5). Note the appearance of peaks spaced at 0.5 m/z intervals in the lower spectrum, characteristic of a doubly charged ion. This observation is entirely consistent with dimerisation from $[\Theta Ag_2I]^-$ to $[\{\Theta Ag_2I\}_2]^{2-}$ ("monomer" meaning species with one Ru_6C core, "dimer" with two). The slight alternation in intensity of the neighbouring peaks in the second pattern is indicative of incomplete dimerisation.

All clusters observed obey the general formula $[\Theta_x Ag_y X_z]^{(2x-y+z)-}$ where $x = 1$ or 2, $y = 1$, 2, 3 or 4 and $z = 0$, 1 or 2. Compounds were identified by isotope pattern matching and by MS/MS studies. Transition metal carbonyl cluster anions tend to fragment in a straightforward fashion by loss of CO ligands, but interesting processes such as
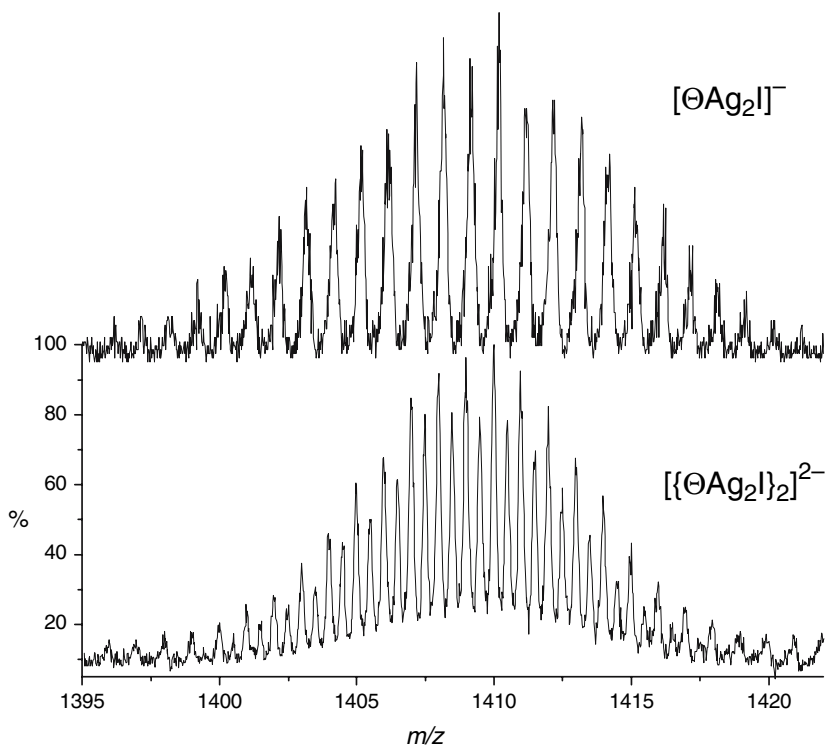

$[\Theta Ag_2I]^-$

$[\{\Theta Ag_2I\}_2]^{2-}$

Fig. 5. Negative-ion ESI-MS from the reaction AgI + $[PPN]_2[\Theta]$; the isotope pattern of the signal centred at 1410 m/z is shown. Top: after 1 h. Bottom: after 2 h.

electron autodetachment [27] and cleaving of the cluster core [28] have been observed to occur for dianions. For this reason, we investigated in particular detail the dianions in the spectrum.

The energy-dependent (ED) ESI-MS/MS of $[\Theta AgI]^{2-}$, the base peak in the mass spectrum of the product mixture (see Fig. 4), was collected and is shown in Fig. 6. EDESI mass spectra involve collecting data over the entire range of available fragmentation energies and presenting this information in the form of a contour map, in which the three dimensions are m/z, collision energy and ion intensity [29]. Fragmentation is caused by collision-induced dissociation (CID) with either N_2 or Ar gas [30].
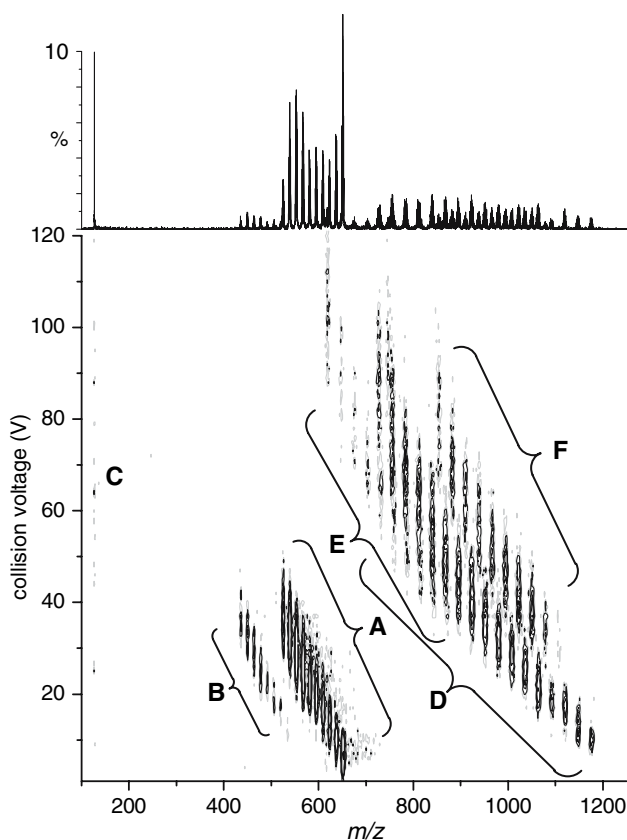
Fig. 6. Negative-ion EDESI-MS/MS of the ion $[\Theta AgI]^{2-}$. A = $[Ru_6C(CO)_nAgI]^{2-}$ ($n = 7$–16),   B = $[Ru_6C(CO)_n]^{2-}$ ($n = 9$–16),   C = I^-,   D = $[Ru_6C(CO)_nAg]^-$ ($n = 0$–16), E = $[Ru_6C(CO)_n]^-$ ($n = 0$–10), F = $[Ru_6C(CO)_nAgI]^-$ ($n = 0$–8).

The spectrum is complicated, but readily explicable. At low collision energy, only the parent dianion is seen, but at very slightly higher energies peaks assignable to three different fragmentation pathways may be observed: (a) loss of CO ligands to produce the series $[Ru_6C(CO)_nAgI]^{2-}$ ($n = 7$–16); (b) loss of I^- to produce the series $[Ru_6C(CO)_nAg]^-$ ($n = 0$–16); (c) loss of AgI to produce the series $[Ru_6C(CO)_n]^{2-}$ ($n = 9$–16). Series (a) and (b), being dianions, undergo electron autodetachment (dianions have a limited existence in the gas phase) [31] to produce the monoanionic series $[Ru_6C(CO)_nAgI]^-$ ($n = 0$–8) and $[Ru_6C(CO)_n]^-$ ($n = 0$–10), respectively. The latter series overlaps with $[Ru_6C(CO)_nAg]^-$ ($n = 0$–16), Ag being approximately equal in mass to $4 \times CO$, so the $[Ru_6C(CO)_n]^-$ ($n = 0$–10) peaks are not immediately discernable in the EDESI map.

Loss of AgI or I^- early in the fragmentation process both suggest that I is *not* bonded to Ru, but only terminally through Ag. This assumption is consistent with electron counting rules, as a bridging halide ligand donates three electrons towards the electron count.

The other especially interesting MS/MS result is the fact that $[\{\Theta Ag_2I\}_2]^{2-}$ breaks apart asymmetrically to form the two monoanions $[\Theta Ag_3I_2]^-$ and $[\Theta Ag]^-$ (Fig. 7).

The first of these appears at 1646 m/z and is also apparent in the mass spectrum of the product mixture, but the second, at 1176 m/z, is not. This observation adds confidence to the assumption that each of the species seen in Fig. 4 is a "real" compound rather than a fragment of some other compound. If $[\Theta Ag_3I_2]^-$ was a fragment, we would expect to see it at the same abundance as $[\Theta Ag]^-$, which is in fact absent from the top spectrum in
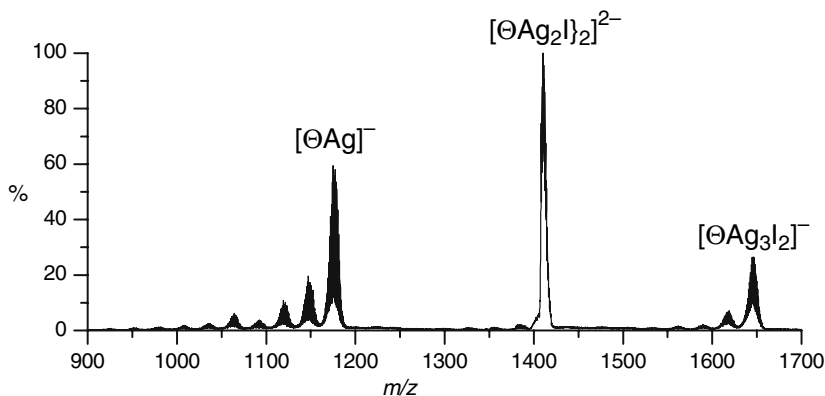

Fig. 7.   Negative-ion ESI-MS/MS of the ion $[\{\Theta Ag_2I\}_2]^{2-}$.

Fig. 4 (though it does appear in trace amounts in the spectrum recorded after 2 min).

The chloride system proved to be almost exactly analogous to the iodide system, with the caveat that peak intensities varied somewhat between the two systems. However, the identity of the base peak in the spectrum and the relative concentration of the ion corresponding to the crystallised product were the same.

Halide exchange

Exchange of halides in this system occurs with great facility, as evidenced by the solid-state structures, and this phenomenon could be tested with ease using ESI-MS. Addition of a small amount of [NMe$_4$]Br to the product mixture from AgCl + [PPN]$_2$[Θ] resulted in significant changes to the mass spectrum (Fig. 8).

The disappearance of all the dimeric species in the spectrum is noteworthy; the spectrum is now dominated by the monomeric compounds [Θ(AgX)$_n$]$^{2-}$ (n = 1 or 2; X = Cl or Br) (and the corresponding 1-ions where the dianion has paired with the NMe$_4$$^+$ counterion). The presence of excess halide has cleaved any halide bridges and removed all species with a superfluity of Ag over X.

The IR spectra and the high yield of the cluster both suggest clean formation of a single product, however, the ESI-MS results suggest that the solution speciation is really very complicated, even after the reaction reaches

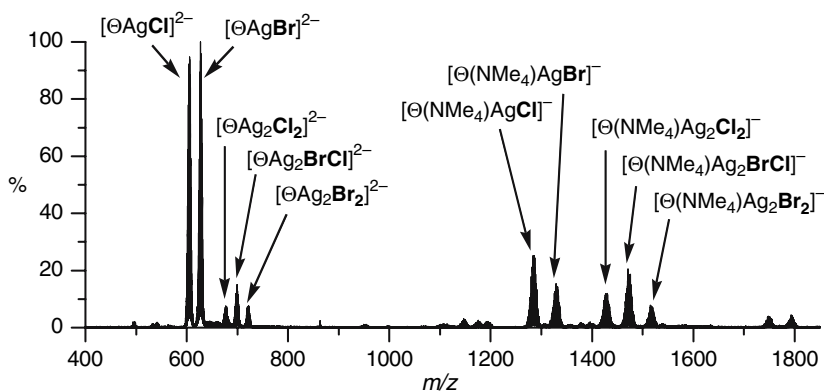**Fig. 8.** Negative-ion ESI-MS of the solution resulting from reaction between AgCl + [Θ]$^{2-}$ after 2 h followed by addition of [NMe$_4$]Br. Note the near-statistical distribution of Br and Cl and the absence of signals due to species with an abundance of Ag over halide.

completion. IR spectra of clusters tend to feature broad, poorly resolved peaks, and Kettle has shown that a spherical approximation of symmetry allows rationalisation of the IR spectra of many higher nuclearity clusters [32]. The mixture of clusters observed in the ESI-MS all share certain characteristics: they all feature the $[\Theta]^{2-}$ core, their overall charge per hexanuclear Ru_6C core is usually 1−, and in cases where the charge is 2−, the second charge is probably largely resident on the remote halide ligand and will have correspondingly little effect on the stretching frequencies of the Ru-bound CO ligands. So we would anticipate the clusters to have IR spectra that closely resembled one another, and the net effect of the mixture would be to have a broad peak with contributions from many clusters with closely similar spectra. There would be a noticeable shift from the starting material, $[\Theta]^{2-}$, as this cluster carries a formal charge of 2− that must be distributed directly on to the CO ligands, moving the average absorption to lower wavenumber. In contrast, $[\Theta AgI]^{2-}$ is able to distribute some of the charge density to the iodide ligand and hence the position of the peak should move to a higher wavenumber.

The ESI-MS shows the crystallographically characterised product to constitute perhaps 10% of the mixture, yet the product was isolated in 80% yield. The identity of the counterion, $[PPN]^+$, *is* different from the $[NBu_4]^+$ used in the crystallographic study, but it is unlikely that this plays a really significant part in affecting the solution speciation. While it may be tempting to acknowledge the fact that ESI-MS peak intensities are an unreliable guide to concentration and attribute the discrepancy accordingly, in our experience the ESI-MS is a reasonably reliable guide to assessing the relative concentrations of different but closely related species in a solution containing a mixture of products [33]. The clue to a better explanation may lie in the observations made in the halide exchange experiment, that is, the rapid attainment of equilibrium, the facile interconversion of a complex mixture of "dimeric" clusters into "monomeric" ones, and of course, the close relationships between the original "complex mixture". In reality, this mixture is dominated to a great extent by clusters that are $[\Theta AgX]^{2-}$ and slight modifications thereof: loss/addition of Ag^+ or X^- and/or dimerisation. It is reasonable to assume that interchange between these species is easy (and indeed, the fragmentation studies carried out using MS/MS point to just how low-energy some of these processes are) and hence, removal of a single species from solution (in this case, by preferential crystallisation) ought to drive the equilibrium in the direction of this particular product. An isolated yield of 80% is perfectly reasonable under this scenario. Redissolution of product will not be expected to yield the same mixture of products, because the absence of an excess of AgX will limit the number of possible products.

Conclusions

Reaction of silver halides with $[Ru_6C(CO)_{16}]^{2-}$ generates linked clusters of formula $[\{Ru_6C(CO)_{16}Ag_2X\}_2]^{2-}$ (X = I or Cl/Br) analogous to the known heteronuclear copper/ruthenium clusters $[\{Ru_6C(CO)_{16}Cu_2Cl\}_2]^{2-}$. ESI-MS reveals that the solution speciation at the completion of this reaction is in fact rather complicated, with a variety of clusters present based on a $[Ru_6C(CO)_{16}Ag]^-$ core, modified with different amounts of Ag^+ and/or Cl^- and present in either monomeric or dimeric form. The high yield of the isolated and crystallographically characterised product, $[\{Ru_6C(CO)_{16}Ag_2X\}_2]^{2-}$, is probably a function of a rapid solution equilibrium being driven by selective crystallisation of the observed product.

REFERENCES

1. (1a) D. Braga, P. Sabatino, P. J. Dyson, A. J. Blake, and B. F. G. Johnson (1994) *J. Chem. Soc. Dalton Trans.* 393. (b) P. J. Dyson, B. F. G. Johnson, J. Lewis, M. Martinelli, D. Braga, and F. Grepioni (1993) *J. Am. Chem. Soc.* **115**, 9062. (c) D. Braga, P. J. Dyson, F. Grepioni, and B. F. G. Johnson (1994) *Chem. Rev.* **94**, 1585. (d) R. D. Adams, B. Captain, W. Fu (2003) *J. Organomet. Chem.* **671**, 158.
2. (2a) R. D. Adams, B. Captain, W. Fu, and M. D. Smith (2002) *J. Am. Chem. Soc.* **124**, 5628. (b) R. D. Adams, B. Captain, W. Fu, M. B. Hall, J. Manson, M. D. Smith, and C. E. Webster (2004) *J. Am. Chem. Soc.* **126**, 5253. (c) R. D. Adams, B. Captain, W. Fu, P. J. Pellechia, and M. D. Smith (2003) *Inorg. Chem.* **42**, 2094. (d) A. B. Hungria, R. Raja, R. D. Adams, B. Captain, J. M. Thomas, P. A. Midgley, V. Golovko, and B. F. G. Johnson (2006) *Angew. Chem. Int. Ed.* **45**, 4782. (e) E. V. Grachova, P. Jutzi, B. Neumann, and H.-G. Stammler (2005) *Dalton Trans.* 3615. (f) T. Khimyak and B. F. G. Johnson (2004) *J. Cluster Sci.* **15**, 543.
3. P. J. Dyson (1999). *Adv. Organomet. Chem.* **43**, 43.
4. L. H. Gade (1993). *Angew. Chem. Int. Ed.* **32**, 24.
5. B. F. G. Johnson, W.-L. Kwik, J. Lewis, P. R. Raithby, and V. P. Saharan (1991) *J. Chem. Soc. Dalton Trans.* 1037.
6. G. B. Ansell, M. A. Modrick, and J. S. Bradley (1984). *Acta Cryst.* **C40**, 1315.
7. T. Nakajima, A. Ishiguro, and Y. Wakatsuki (2001). *Angew. Chem. Int. Ed.* **40**, 1066.
8. M. A. Beswick, J. Lewis, P. R. Raithby, and M. C. Ramirez de Arellano (1996) *J. Chem. Soc. Dalton Trans.* 4033.

9. D. S. Shephard, T. Maschmeyer, G. Sankar, J. M. Thomas, D. Ozkaya, B. F. G. Johnson, R. Raja, R. D. Oldroyd, and R. G. Bell (1998). *Chem. Eur. J.* **4**, 1214.

10. (a) R. D. Adams and W. Wu (1991) *J. Cluster Sci.* **2**, 271. (b) P. J. Bailey, A. J. Blake, P. J. Dyson, B. F. G. Johnson, J. Lewis, and E. Parisini (1993) *J. Organomet. Chem.* **452**, 175. (c) P. J. Dyson (2002) *Appl. Organomet. Chem.* **16**, 495.

11. D. S. Shephard, T. Maschmeyer, B. F. G. Johnson, J. M. Thomas, G. Sankar, D. Ozkaya, W. Zhou, R. D. Oldroyd, and R. G. Bell (1997). *Angew. Chem. Int. Ed.* **36**, 2242.

12. S. Hermans, T. Khimyak, N. Feeder, S. J. Teat, and B. F. G. Johnson (2003) *Dalton Trans.* 672.

13. R. D. Adams and B. Captain (2004). *J. Organomet. Chem.* **689**, 4521.

14. J. M. Thomas, B. F. G. Johnson, R. Raja, G. Sankar, and P. A. Midgley (2003). *Acc. Chem. Res.* **36**, 20.

15. D. Braga, F. Grepioni, P. J. Dyson, B. F. G. Johnson, P. Frediani, M. Bianchi, and F. Piacenti (1992), *J. Chem. Soc. Dalton Trans.* 2565.

16. S. Hermans, T. Khimyak, and B. F. G. Johnson (2001) *J. Chem. Soc. Dalton Trans.* 3295.

17. (a) P. J. Dyson, N. Feeder, B. F. G. Johnson, J. S. McIndoe, and P. R. R. Langridge-Smith (2000) *J. Chem. Soc. Dalton Trans.* 1813. (b) S. L. G. Husheer, O. Forest, M. Henderson, and J. S. McIndoe (2005) *Rapid Commun. Mass Spectrom.* **19**, 1352. (c) E. Crawford, P. J. Dyson, O. Forest, S. Kwok, and J. S. McIndoe (2006) *J. Cluster Sci.* **17**, 47.

18. Oxford Diffraction Ltd, Abingdon, OX144 RX, UK, CrysAlis RED.

19. G. M. Sheldrick, *SHELX-97. Structure Solution and Refinement Package* (Universität Göttingen, 1997).

20. SHELXTL97, *Structure Solution and Refinement Package* (Universität Göttingen, Göttingen, 1997).

21. N. Walker and D. Stuart (1983). *Acta Crystallogr. A.* **39**, 158.

22. Diamond 3.0a, Crystal Impact GbR, Bonn, Germany.

23. J. S. Bradley, R. L. Pruett, E. Hill, G. B. Ansell, M. E. Leonowicz, and M. A. Modrick (1982). *Organometallics* **1**, 748.

24. (a) T. Chihara and H. Yamazaki (1995) *J. Chem. Soc. Dalton Trans.* 1369. (b) P. J. Dyson, S. L. Ingham, B. F. G. Johnson, J. E. McGrady, D. M. P. Mingos, and A. J. Blake (1995) *J. Chem. Soc. Dalton Trans.* 2749. (c) A. J. Blake, A. Harrison, B. F. G. Johnson, E. J. L. McInnes, S. Parsons, D. S. Shephard, and L. J. Yellowlees (1995) *Organometallics* **14**, 3160.

25. (a) S. A. Hofstadler, R. Bakhtiar, and R. D. Smith (1996) *J. Chem. Educ.* **73**, A82. (b) J. B. Fenn, M. Mann, C. K. Meng, S. F. Wong, and C. M. Whitehouse (1990) *Mass Spec. Rev.* **9**, 37. (c) J. B. Fenn, M. Mann, C. K. Meng, S. F. Wong, and C. M. Whitehouse (1989) *Science* **246**, 64. (d) W. Henderson and J. S. McIndoe, *Mass Spectrometry of Inorganic and Organometallic Compounds* (John Wiley & Sons, Chichester, 2005).

26. (a) Y.-Y. Choi and W.-T. Wong (1999) *J. Chem. Soc., Dalton Trans.* 331. (b) W. Henderson, L. J. McCaffrey, and B. K. Nicholson (1998) *Polyhedron* **17**, 4291. (c) D. J. F. Bryce, P. J. Dyson, B. K. Nicholson, and D. G. Parker (1998) *Polyhedron* **17**, 2899. (d) M. Ferrer, R. Reina, O. Rossell, M. Seco, and G. Segales (1996) *J. Organomet. Chem.* **515**, 205. (e) W. Henderson and B. K. Nicholson (1995) *Chem. Commun.* 2531. (f) R. Colton, A. D'Agostino, and J. C. Traeger (1995) *Mass Spec. Rev.* **14**, 79. (g) P. J. Dyson, B. F. G. Johnson, J. S. McIndoe, and P. R. R. Langridge-Smith (2000) *Inorg. Chem.* **39**, 2430. (h) B. F. G. Johnson and J. S. McIndoe (2000) *Coord. Chem. Rev.* **200–202**, 901. (i) C. Evans, K. M. Mackay, and B. K. Nicholson (2001) *J. Chem. Soc. Dalton Trans.* 1645.

27. C. P. G. Butcher, B. F. G. Johnson, J. S. McIndoe, X. Yang, X. -B. Wang, and L. -S. Wang (2002). *J. Chem. Phys.* **116**, 6560.

28. C. P. G. Butcher, P. J. Dyson, B. F. G. Johnson, T. Khimyak, and J. S. McIndoe (2003). *Chem. Eur. J.* **9**, 944.

29. (a) P. J. Dyson, B. F. G. Johnson, J. S. McIndoe, and P. R. R. Langridge-Smith (2000) *Rapid Commun. Mass Spectrom.* **14**, 311. (b) P. J. Dyson, B. F. G. Johnson, J. S. McIndoe, P. R. R. Langridge-Smith, and C. Whyte (2001) *Rapid Commun. Mass Spectrom.* **15**, 895. (c) C. P. G. Butcher, P. J. Dyson, B. F. G. Johnson, P. R. R. Langridge-Smith, J. S. McIndoe, and C. Whyte (2002) *Rapid Commun. Mass Spectrom.* **16**, 1595.

30. S. A. McLuckey (1991). *J. Am. Soc. Mass Spectrom.* **3**, 599.

31. (a) X.-B. Wang and L.-S. Wang (1999) *Phys. Rev. Lett.* **83**, 3402. (b) L.-S. Wang and X.-B. Wang (2000) *J. Phys. Chem. A* **104**, 1978.

32. (a) S. F. A. Kettle, E. Diana, R. Rossetti, and P. L. Stanghellini (1997) *J. Am. Chem. Soc.* **119**, 8228. (b) S. F. A. Kettle, E. Diana, R. Rossetti, and P. L. Stanghellini (1998) *Inorg. Chem.* **37**, 6502.

33. P. J. Dyson, A. K. Hearley, B. F. G. Johnson, J. S. McIndoe, and P. R. R. Langridge-Smith (2001). *Organometallics* **20**, 3970.